Strojniški vestnik - Journal of Mechanical Engineering 56(2010)7-8, 436-446
UDC UDK 629.734.33:351.814.343
Paper received: 10.12.2007
Paper accepted: 02.07.2010

Analysis of the Sailplane Final Approaches Performed by Cosine-Law Speed Variations

Zoran Stefanović - Ivan Kostić*
University of Belgrade, Faculty of Mechanical Engineering, Serbia

High lift-to-drag ratios of the contemporary sailplanes make them the most energy efficient flying vehicles. On the other hand, this capability may become their serious disadvantage during the landing, if their aerodynamic deceleration devices become inoperable in flight. Not being able to dissipate the excess energy quickly when close to the ground, they may fly over the available landing ground and finish up in front of the obstacles, with still too much energy to land and not enough to fly over them.

Beside the sideslipping flight in final, where energy is dissipated through the increased sideforce drag, another solution to this problem has been offered in a number of papers. By numerical analyses they have shown that landing distance in such cases could be minimized using rather complex oscillating flight paths in vertical plane. Although relevant distance reductions could be achieved through them, performing such paths in practice would require exceptional piloting skills. Instead of that, in this paper much simpler approach profiles have been analyzed, based on two types of cosine speed variations with constant periods and amplitudes, which could be flown by pilots of average flying experience. After establishing a quick convergence algorithm, numerical solutions for several typical cases, belonging to two general speed variation types, have been presented. The same initial and terminal reference energy states have been used. Although the distance reductions are smaller than obtained by distance-minimizing techniques, operational simplicity of presented techniques and some specific advantages prove them valuable within this category of problems.

Keywords: sailplane, final approach, inoperable spoilers, cosine speed variations

0 INTRODUCTION

Modern sailplanes have very high glide ratios, and due to that they are able to fly very long distances without a power plant, loosing proportionally small height at the same time. This makes them extremely energy-efficient flying vehicles. Since the available landing grounds (runways, or sometimes just long enough countryside fields) are often limited by obstacles on both ends, sailplane pilots generally perform their final landing approaches at much steeper angles than during the gliding flight. This is normally done with spoilers extended, which increase drag, partially reduce lift and increase the dissipation of energy. Quick reduction of height is achieved without remarkable increase of the sailplane's speed. But the final approach can be one of the most critical phases of a sailplane flight if, for any technical reason, spoilers or other available aerodynamic deceleration devices become inoperable (cases which do not happen often, but are known in practice). With the nose pointed rather steeply down to clear an obstacle and aim for the beginning of the landing ground, a sailplane will very rapidly gain too much speed and simply "refuse to land". Forcing it down to the ground at too high speed will make it bounce-off and, at worst, may lead to a crash landing. On the other hand, if patiently waiting for a sailplane to slowly decelerate above the ground, a pilot may fly over the available landing area and finish up facing the obstacles, neither being able to land in front of them, nor to fly over them.

One of the known operational techniques that can be used to face this problem is the sideslipping during the final approach phase. During such an intentionally uncoordinated flight, additionally generated sideforce will increase the overall drag. Principally like with spoilers, this drag component will also dissipate additional quantity of energy and shorten the approach distance. But this technique requires a certain amount of skill. For example, in case of a not too experienced pilot forced to land on a narrow countryside field, improper estimation of the

*Corr. Author's Address: University of Belgrade, Faculty of Mechanical Engineering, Aeronautical Department, Kraljice Marije 16, 11120 Belgrade, Serbia, ikostic@mas.bg.ac.rs

actual flight direction while watching over his shoulder, in this maneuver may finally place him in front of a wrong field, with no engine to help him go around and correct the error.

Beside this classical technique, in a certain number of papers the oscillating final approach patterns without sideslipping, performed in a vertical plane, have been considered as another potential option with an aim to *minimize* the landing distance in case of the aerodynamic decelerating devices failure. In order to emphasize a rather high complexity level of such kind of calculations, one of them performed for the Vuk-T sailplane [1] will be described very briefly. It treated the problem of minimizing the landing approach distance as an optimal control problem, where the initial and the terminal states were based on recommendations from [2]. In these papers the lift coefficient variation was established as a variable of the control function $u(t)$ according to [3] and the maximum lift coefficient value of 1.78 for the Vuk-T. Since the total time of the final approach, originally denoted as t_k, is initially unknown, calculations were done in normalized time τ, introducing another control parameter α, where $t = \alpha \cdot \tau$, $0 \le t \le t_k$, and $0 \le \tau \le 1$. Path for the minimum landing distance was obtained through an iterative calculation process, were the point was to determine such function $u(t)$ and an α that will minimize the so called performance index I, which is subjected to the dynamic, initial and terminal state constraints. Index I included the integral interior penalty functions [4] for the minimum speed and the height constraints, combined by the empirical fixed constraint factors. The problem was solved using a gradient projection algorithm [5], which incorporated conjugate directions of search for a rapid convergence of the solution. Those calculations were done in Fortran 77 in double precision mode. Flight path of the so minimized approach distance and the appropriate lift coefficient are shown in Fig. 1.

Advantages of such an approach are the effective reduction of the approach distance and the fact that, during this phase of flight, the nose of a sailplane is permanently pointed in the direction of intended landing area. On the other hand, this obviously quite complex calculation gives as a result an unevenly oscillating flight profile. Such approach path could be rather difficult both for memorizing and for performing under the operational flight conditions. If several errors were accumulated during such final approach (and hoping that the sailplane would not be accidentally stalled in the final stages, flying at very small speeds in the vicinity of the ground), the sailplane could land further from the initially estimated touchdown point. If a pilot is forced to land on a rather short field, this might be equally critical as a potential directional misjudgment, mentioned in case of the sideslip landings on narrow fields.

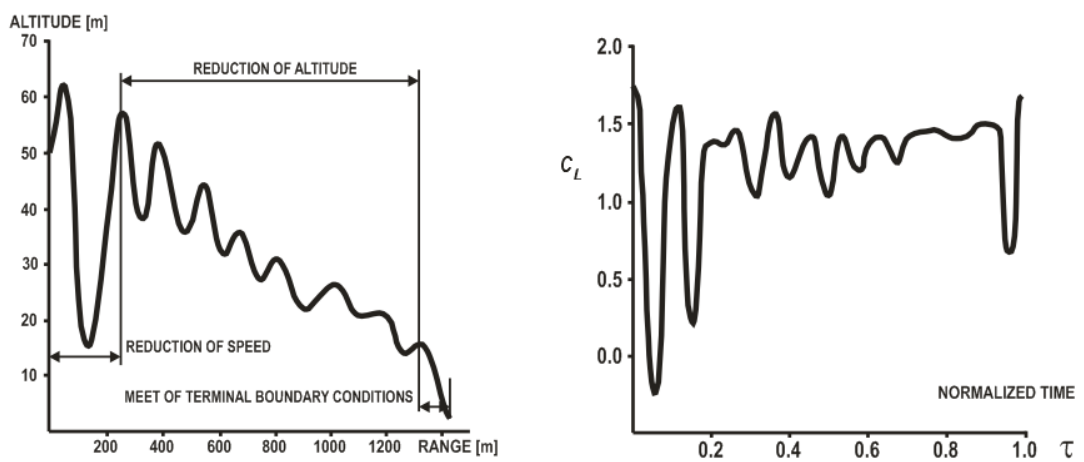

Fig. 1. *Example of a rather complex approach profile for the minimized approach distance and the corresponding lift coefficient, calculated for the Vuk-T sailplane [1]*

As a contrast to previously described method, the aim of this paper is to investigate *very simple periodical flight path changes* in the vertical plane without sideslipping, and the final approach distance reductions that could be achieved through them, also assuming that spoilers are inoperable. The primary goal is that such flight paths could sufficiently accurately and easily be flown by the pilots of average flying skills, using just two instruments that are always on board: a speed indicator and a stop or a wrist watch. The predefined cosine harmonic approach speed variations, divided in two general categories, all with constant amplitudes and periods, have been selected as a good mathematical resemblance of the pilot's natural control inputs in attempt to evenly "pump" the flight speed up and down. In order to preserve compatibility with the previous example, the Vuk-T sailplane has also been selected for actual calculations, subjected in all cases to the same initial conditions and input parameters as in [1].

Another very important aim of this paper is to keep the calculation model as simple as possible, but efficient and sufficiently accurate for the required purposes. It is clear that the potential end users of this calculation model would mostly likely be the amateur sailplane pilots - who are generally not experts in advanced programming, rather than highly trained engineers. Thus, if these calculations are kept simple enough, they could be incorporated in some of the available commercial software, like spreadsheet programs, which do not require highly sophisticated coding or recompiling. In that case, a pilot with only the general knowledge of informatics could perform even major program editing, for example, by experimenting with the different laws of speed variations, or making combinations of several simple paths in one approach, etc. Necessary input data could be obtained from the sailplane manufacturers, operation manuals supplied with the sailplanes, or from other available sources.

Such calculations should help pilots to define parameters of several possible final approach paths for the sailplane types which they fly, considering possible field position and length, general obstacle distribution, etc., and estimate in advance the approach distances in case that spoilers become inoperable. Memorizing the speed amplitudes, periods and expected approach distance reductions, chances of making misjudgments considering the direction or distance in final approach should be much smaller. On the other hand, the price for increased safety using the techniques that will be presented in the following chapters is that the approach distance reductions will most probably be smaller than in case of the other two mentioned techniques.

1 ALGORITHM OF CALCULATIONS

The sailplane configuration in final approach for these calculations is gear-down and spoilers-in. According to the flight test measurements performed on the Vuk-T sailplane prototype, at the Flight Test Center VOC-Batajnica (which just slightly differed from the production sailplanes such as the one shown in Fig. 2), polar for this configuration is defined by equation:

$$C_D = 0.01756 - 0.0095\,C_L + 0.021\,C_L^{\,2}, \qquad (1)$$

where C_D and C_L are drag and lift coefficients, respectively.

Fig. 2. *Vuk-T of the Ljubljana aero-club*

As in [1], in this paper it is also assumed that the nominal mass of the sailplane in flight is $m = 320\,\text{kg}$, and that the air density is $\rho = 1.225\,\text{kg/m}^3$. Aerodynamic wing area of this sailplane is $S = 12\,\text{m}^2$. Using these values and Eq. (1), it can be easily calculated that maximum glide, or L/D ratio for this sailplane configuration is $(L/D)_{\max} = 34.59$ at the speed of $V = 77.99\,\text{km/h}$ (values for gear-up configuration are different; also, this velocity is additionally influenced by the assumed mass). For the default

glide regime, which will be used for comparison with approaches based on cosine velocity variations, the rounded value of $V = 80$ km/h will be applied, for which $L/D = 34.52$.

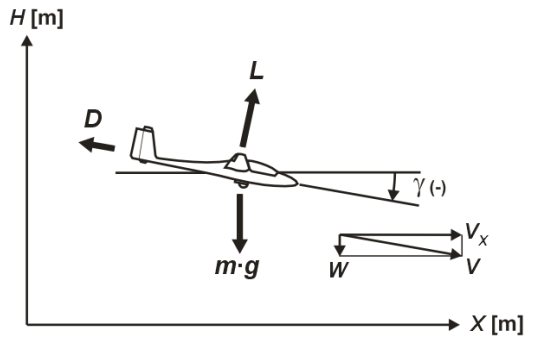

Fig. 3. *Forces and velocity components in descent*

Neglecting the rotation dynamics and assuming that the wind speed is equal to zero, equations of motion [6] for the purpose of these calculations (see also Fig. 3) can be written as:

$$m\frac{dV_X}{dt} = -D\cos\gamma - L\sin\gamma\,, \tag{2}$$

$$m\frac{dW}{dt} = -mg - D\sin\gamma + L\cos\gamma\,, \tag{3}$$

$$\frac{dX}{dt} = V_X\,, \tag{4}$$

$$\frac{dH}{dt} = W\,, \tag{5}$$

$$\tan\gamma = \frac{W}{V_X}\,, \tag{6}$$

where:

$$L = C_L \cdot \frac{1}{2}\rho V^2 \cdot S\,, \tag{7}$$

$$D = C_D \cdot \frac{1}{2}\rho V^2 \cdot S\,. \tag{8}$$

In this paper, the speed variations in final approach will be assigned as inputs that can be divided in two general categories, depending on which of the following two equations is applied:

$$V = V_{AV} - \Delta V\cos\left(\frac{2\pi}{T}t\right), \tag{9}$$

$$V = V_{AV} + \Delta V\cos\left(\frac{2\pi}{T}t\right), \tag{10}$$

where V_{AV} represents the average speed, ΔV is the half-amplitude, T is the period, while time t is the independent variable. For example, if we substitute $V_{AV} = 85$ km/h, $\Delta V = 5$ km/h and $T = 17$ s in Eq. (9), the initial speed at $t = 0$ s is 80 km/h, at $t = 8.5$ s speed increases to 90 km/h, while at the $t = T = 17$ s it is be 80 km/h again. In contrast to that, the application of Eq. (10) will lead to the initial speed decrease.

In order to achieve quick convergence of the solution, calculations have been performed in several iteration steps, with complexity and accuracy levels increasing gradually from one step to another. Also, in calculations aimed for engineering and practical purposes, small angle approximations can be applied for values of the glide path angle $\gamma < 10^{\circ}$, but obtained solutions must be finally substituted into the full equations for the verification of the achieved accuracy. Thus, with γ expressed in radians, Eqs. (2) and (3) can be written as:

$$m\frac{dV_X}{dt} = -D - L\cdot\gamma\,, \tag{11}$$

$$m\frac{dW}{dt} = -mg - D\cdot\gamma + L\,. \tag{12}$$

It should be noted that all variables on the right hand-side of Eqs. (2) or (3), or (11) and (12), with the speed changing according to an assigned law, will also be time dependant (except the sailplane weight $m\cdot g$).

In the first iteration step, the lift coefficient variation with time along the flight path is initially estimated from the equation:

$$C_L(t) = \frac{2\cdot m\cdot g}{\rho\cdot V(t)^2\cdot S} \tag{13}$$

using Eq. (9) or (10) to define speed changes. After that, the time dependant drag coefficient is calculated using Eq. (1). Both in this and the following iterations, a time step of $\Delta t = 0.1$ s for the numerical analyses proved to be quite satisfactory. It should be noted that the Eq. (13) is actually obtained from Eq. (12), omitting the product $D\cdot\gamma$ and assuming that $dW/dt = 0$. In usual sailplane descents, products $D\cdot\sin\gamma$ are

about 1000 times smaller than $L \cdot \cos\gamma$, thus omitting $D \cdot \gamma$ does not affect the accuracy noticeably. On the other hand, for here applied cosine speed changes, the assumption $dW/dt = 0$ is not true, but has been taken as an intentional "sacrifice" in the initial stage of the calculations.

Lift and drag forces are then calculated using Eqs. (7) and (8). To a first approximation, we can say that $dV_X/dt \approx dV/dt$. Since the variation of $V(t)$ is a known differentiable function, dV/dt can be obtained both numerically and analytically (doing it both ways and comparing the results might be one of the verifications whether Δt is selected adequately). The initial estimate of the flight path angle γ can now be obtained directly from Eq. (11):

$$\gamma(t) = -\frac{m(dV/dt) + D(t)}{L(t)}. \tag{14}$$

Knowing these values, the velocity components are determined as:

$$V_X(t) = V(t) \cdot \cos\gamma(t), \tag{15}$$

$$W(t) = V(t) \cdot \sin\gamma(t). \tag{16}$$

In the sense of numerical calculations, their time derivatives at the i^{th} time step are obtained as:

$$\left(\frac{dV_X}{dt}\right)_i = \frac{(V_i - V_{i-1}) + (V_{i+1} - V_i)}{2 \cdot \Delta t}, \tag{17}$$

$$\left(\frac{dW}{dt}\right)_i = \frac{(W_i - W_{i-1}) + (W_{i+1} - W_i)}{2 \cdot \Delta t}. \tag{18}$$

In the second iteration step, the lift coefficient Eq. (13) is upgraded, this time including values obtained from (18):

$$C_L(t) = \frac{2 \cdot m \cdot (g + dW/dt)}{\rho \cdot V(t)^2 \cdot S}, \tag{19}$$

while Eq. (14) is upgraded using the values obtained by Eq. (17):

$$\gamma(t) = -\frac{m(dV_X/dt) + D(t)}{L(t)}. \tag{20}$$

Lift, drag, and the velocity components with their derivatives are then recalculated applying the same algorithm as in the first iteration step, but including the refined values obtained using Eqs. (19) and (20).

In the third iteration step the whole procedure is repeated, this time using dV_X/dt and dV/dt from the second step, etc; this calculation process can be repeated as many times as necessary, until the desired accuracy is achieved.

The $X(t)$ and $H(t)$ coordinates, which determine flight path profile, are calculated by numerical integration of the $V_X(t)$ and the $W(t)$ from the last iteration step with respect to time (coming out from Eqs. (4) and (5)), using initial conditions $X(0)$ = 0 m and $H(0)$ = 50 m for all cases considered in this paper. The length of the flight path $P(t)$ is obtained by numerical integration of the total velocity $V(t)$.

To quantify the obtained accuracy, results from the last iteration step were substituted in full Eqs. (2) and (3). Differences between the left and the right-hand sides, calculated at each time step, were then compared with the calculated drag force in case of Eq. (2) and lift force in case of Eq. (3). Limit for so defined relative errors, which could be accepted for practical considerations, was established at the order of 1% or smaller. The presented algorithm has shown very high convergence rate, since practically all analyzed cases with the cosine speed variations have fulfilled this requirement after only three iteration steps. The only exception was case denoted as "I-2" (see Chapter 2, Fig. 7), where the fourth step was introduced to reduce the maximum relative error from 2.2 to 1.2% in Eq. (2). Since the differences between the calculated X and H values in the third and fourth step in this case were of the order of centimeters, it has been assumed that any further accuracy improvements would not be necessary.

Terminal state is reached at the $H \approx 1$ m and V = 72 km/h. Thus, beside the final approach, the round-out phase and the hold-off phase (Fig. 4) also had to be calculated for the default case and case I-3 (chapter 2, Figs. 5 and 8). For all other approaches the velocity amplitudes and the corresponding periods have been selected in a way that the round-out phase is an integral part of the final approach path.

For usual landings ((A) in Fig. 4), the round-out phase is often modeled as a circular arc i.e. R = const., through which the approach speed V_{AP} changes are practically negligible. On the other hand, changes of the load factor $n = L/(m \cdot g)$ are not.

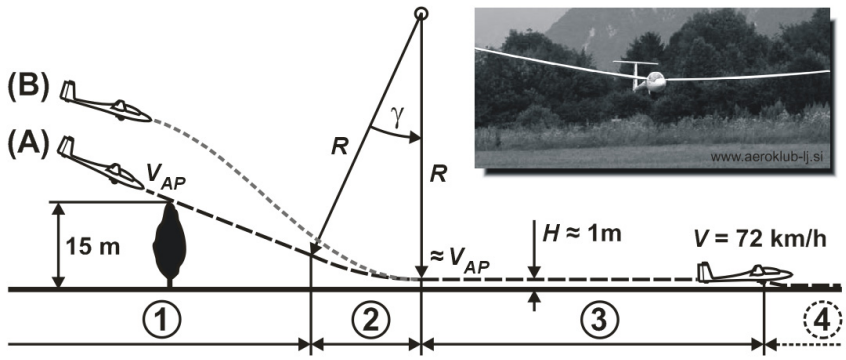

Fig. 4. *Usual landings (A) consist of: (1) the final approach with $\gamma \approx$ const., (2) the round-out phase, (3) the hold-off phase and (4) the landing run (not considered in this paper); in here analyzed cosine approaches (B), phase (2) is integral part of the phase (1) for which $\gamma \neq$ const.*

Radius of such modeled round-out phase can be determined from the equation:

$$R = \frac{V_{AP}^{\ 2}}{g} \cdot \frac{1}{n - \cos\gamma}, \tag{21}$$

where n is the load factor at the end of this phase. For both mentioned cases, $n = 1.05$ has been assumed. Total variations of the height and the horizontal distance through the round-out phase are:

$$\Delta H = -R(1 - \cos\gamma), \tag{22}$$

$$\Delta X = -R\sin\gamma. \tag{23}$$

The hold-off phase has been modeled in the same way for all analyzed cases, through which the speed is gradually reduced to the intended touchdown value of $V_T = 72$ km/h. (For $m = 320$ kg, the Vuk-T's stalling speed is $V_{stall} = 55.7$ km/h; it should be noted that, for many sailplanes, decelerating to V_{stall} would lead to the tail-first touchdowns, which can cause damage to the structure). Although under operational conditions there is usually a small loss of height through this phase and strictly speaking vertical velocity component $W \neq 0$, for practical analyses the equation of level flight with center of gravity at a constant average height $H \approx 1$ m can readily be used. Substituting $\gamma = 0^o$ in Eq. (2), it becomes:

$$m\frac{dV_X}{dt} = -D = m\frac{dV}{dt}, \tag{24}$$

and thus:

$$\frac{dV}{dt} = -\frac{\rho \cdot V^2 \cdot C_D \cdot S}{2m}. \tag{25}$$

Initial condition is defined by V at the end of round-out phase (in the next chapter parameters at this point will be denoted using the symbol "(*)"), and for each consecutive time step speed reduction is calculated using Eq. (25). The new C_L for the reduced speed is obtained from the equation of level flight, while the corresponding C_D is calculated using Eq. (1). The calculation continues until $V_T = 72$ km/h is reached. Distance X flown in this phase is obtained by the integration of speed with respect to time, and for this phase horizontal distance is equal to the path length, $X = P$. The ground roll after touchdown has not been considered because, after the common terminal state parameters have been reached, ground roll for all analyzed cases would be the same for the same terrain categories and qualities.

2 SELECTED CASES AND RESULTS

It is usual to assume that, before commencing a final approach, the sailplane would most probably fly at the speed close to that of the maximum glide ratio. As derived in the previous chapter, this value for the Vuk-T in the gear-down and spoilers-in configuration and $m = 320$ kg is about 80 km/h. The final approaches are usually commenced at about $H = 50$ m above the terrain, so these values, similarly as in [1], will define the initial (energy) state for all considered cases. Also, based on the

sources mentioned in the introduction, the speed of 20 m/s, i.e. 72 km/h for the same sailplane mass, and the center of gravity height of 1 m above the ground, have been selected to define the terminal (energy) state for all cases.

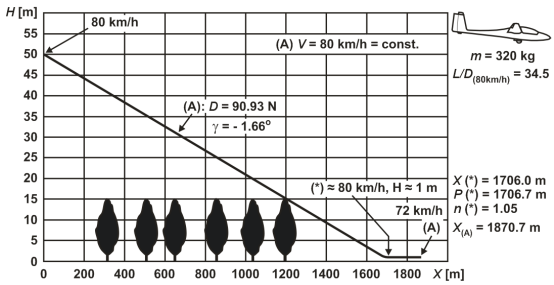

Fig. 5. *Default path - steady glide*

As a reference, or a default case for all comparisons, a steady descent with linear approach path at a constant speed of 80 km/h has been selected (Fig. 5). On the other hand, it is well known that while flying at the speed of the best glide ratio, a sailplane will achieve the longest possible range from a certain height (which is, by the way, quite opposite from the pilot's intentions while attempting to land on a short field and the spoilers are not in function). At both higher and lower speeds, the range will always be smaller. So a question may arise - why select the best glide ratio speed for a reference, when all other constant speed approaches used as a reference would give steeper glide paths and more rigorous critics of here considered paths with cosine speed variations? Just partial, but hopefully sufficient answer could be that at the same height of $H = 50$ m but different initial speeds, a sailplane will have the same potential energy, but different kinetic energies, or in other words, the different flight histories before reaching 50 m height. If we want to quantify the potentials of a certain flight profile to dissipate energy more effectively then some reference profile, both (1) their *initial* energy states, on one side, and (2) their *terminal* states on the other, must be *the same* for the comparison purposes. While many other reasonable reference speed choices can satisfy the second requirement owing to the deceleration (as much as necessary) within the hold-off phase, a steady reference path with the approach speed of 80 km/h is the only one that satisfies the first requirement.

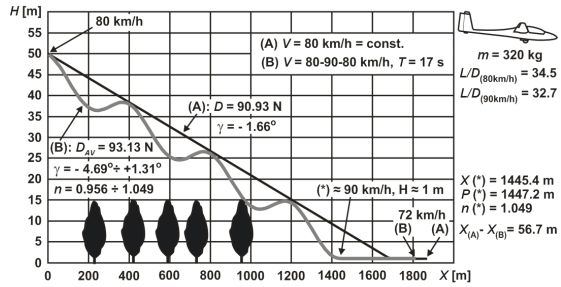

Fig. 6. *Case I-1*

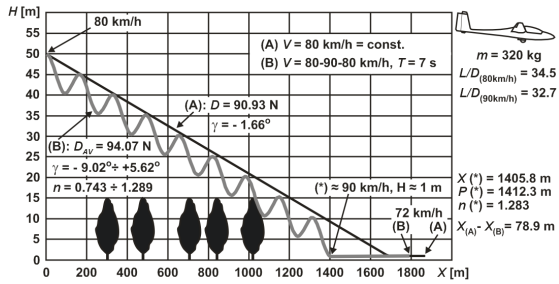

Fig. 7. *Case I-2*

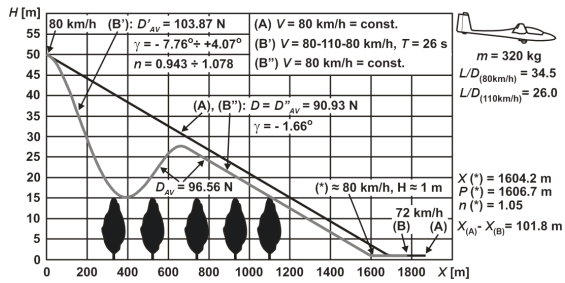

Fig. 8. *Case I-3*

Several typical cases selected for the presentation and analyses in this paper are shown in Figs. 6. to 10. Those within the category "case I-..." are based on the application of Eq. (9), while those named as "case II-..." are obtained using Eq. (10). Numerical example from the previous chapter, with speed variations between 80 and 90 km/h and $T = 17$ s, corresponds to the flight path shown in Fig. 6. The reference path is marked with "(A)", while all paths with cosine speed variations are denoted as "(B)". The tree symbols represent standard 15 meters obstacles.

The most important results, necessary for the discussions in the next chapter, are presented within the figures. Values $X(*)$ and $P(*)$ are the horizontal distance flown and the actual flight path length at the end of the round out phase,

respectively; D_{AV} is the distance-averaged drag force along the cosine final approach segment, not including hold-off; n shows the range of the load factor variations in cosine approaches; γ denotes the extreme path angle variations, etc. Parameters of the cosine law speed variations, influenced by the sailplane type and its actual mass in flight, have been carefully selected as easy-to-remember *rounded numbers* considering the speed variations and the periods. They also had to satisfy the terminal height conditions with the round number of cycles for the paths based on Eq. (10), and round number +1/2 cycles when Eq. (9) was applied. In cases II-1 and II-2, only for theoretical considerations, the periods of the order of $T \approx 20$ were spread to the first decimal accuracy in order match the terminal 1 m height with some ±5 cm accuracy obtained in other cases.

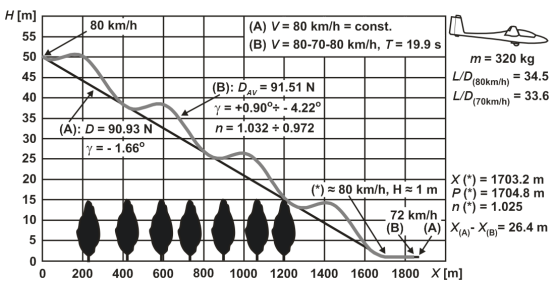

Fig. 9. *Case II-1*

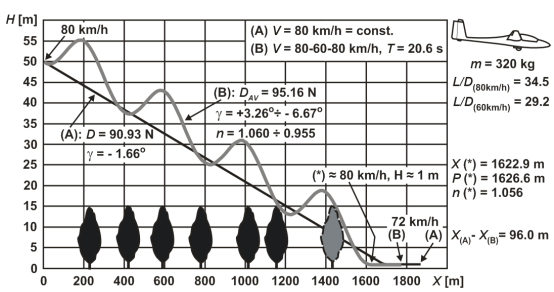

Fig. 10. *Case II-2*

Although the calculations considering here presented subject have initially been done using a custom written Fortan code, a parallel effort has been made to obtain the results in one of the most commonly used spreadsheet programs, the MS Excel. Owing to a reasonable simplicity and high convergence rate of the applied algorithm, the spreadsheet version has also proven to be highly functional.

3 DISCUSSION OF THE RESULTS

Let us first comment an issue which considers the oscillatory approach path profiles. Looking at the Figs. 6 to 10, it may seem that the length along an oscillating path between the two points in final approach should be substantially longer than the straight-line distance between them. Thus, the first impression might be that just by shrinking a straight line into an oscillating path profile could, by itself, contribute to the decrease of the landing distance. On the other hand, relatively small differences even between the $X(*)$ and the $P(*)$ shown in these figures, suggest quite opposite. It should be noticed that, for the clarity of the presentation, scales for X and H had to be remarkably different (paths with γ shown in figures would correspond to the $L/D \approx 1.6$), thus the true appearances of the sailplane paths are largely distorted. That could be understood better by comparing Figs. 8. and 11, or by "manually" checking the default path length (neglecting the round-out phase curvature): $P(*) \approx \sqrt{1706^2 + 49^2} = 1706.7$ m, while $X(*) = 1706.0$ m (see Fig. 5). Thus the oscillating path profiles, by themselves, can not cause any relevant X distance reductions in here presented cases (more detailed explanation, which can be generalized to all such flight paths, can be found in [7]), so attention should be focused primarily on the drag force.

Fig. 11. *True appearance of the case I-3, with H and X coordinates drawn in the same scale*

Dissipation of energy in sailplane descents is achieved through the work done by the drag force along the flight path. Since the prescribed initial and terminal energy states for all analyzed cases are exactly the same, an increase in the drag force with respect to a steady approach case must induce a proportional decrease of the flight path length P and consequently the decrease of the horizontal distance X between the initial and the terminal point.

Table 1. *Review of the most important landing profile parameters*

1	2	3	4	5	6
Case	D_{AV} [N]	$\Delta X = X_A - X_B$ [m]	ΔV [km/h]	$\Delta(L/D)$	T [s]
Default case	90.9	0	0	0	/
Case II-1	91.5	26.4	- 10	- 0.9 (-2.6%)	19.9
Case I-1	93.1	56.7	+ 10	- 1.8 (-5.2%)	17
Case I-2	94.1	78.9	+ 10	- 1.8 (-5.2%)	7
Case II-2	95.2	96.0	- 20	- 5.3 (-15.4%)	20.6
Case I-3	96.6 (103.9)*	101.8	+ 30	- 8.5 (-24.6%)	26

* *Actually, the value denoted as D_{AV}' is the true generator of ΔX for case I-3, since its second part is equivalent to the default path, just shifted to the left.*

For all cases the varying drag force has been integrated along the final approach and the round-out phases with respect to the path length, and then divided by the total path length of these two landing segments. This way, the distance-averaged drag forces D_{AV} in approach have been obtained. The previously mentioned principle can be confirmed if these values are compared with the achieved distance reductions ΔX, as shown in Table 1.

From Table 1 it is also obvious that the larger speed deviations ΔV from the initial state velocity of 80 km/h generally correspond to higher ΔX values. Remembering that the selected initial speed is practically the maximum glide ratio speed for the given configuration and mass, any diverging from it must cause the decrease of the glide ratio (Table 1, col. 5). This causes increased drag for the same amount of lift and, as a final consequence, shorter flight path. (If some other speed is selected for the initial state, then varying the velocity in the opposite "direction" from the $(L/D)_{MAX}$ speed will lead to the decrease of the approach distance, and vice versa). Knowing that, a logical question might be - why the flight path should be oscillating at all, when a much simpler procedure, based on the continuous speed increase in final approach (let us say from 80 to 90 km/h), will decrease the L/D ratio and probably also lead to the decrease of the landing distance? Such an approach has been analyzed in [7], setting the period to $T = 120$ s and using just half of the cycle based on Eq. (9). After the round-out and hold-off phases had been added, the ΔX reduction of some 33 m was achieved, compared to the default path. On the other hand, in cases I-1 and I-2, where speed variations were also between 80 and 90 km/h, the distance reductions were 56.7 m ($T = 17$ s) and 78.9 m ($T = 7$ s), respectively. It implies that, for the same speed amplitude, shorter periods (more oscillations) generate larger landing distance reductions.

In an attempt to explain this particular phenomenon, let us compare load factor variations about the value $n = 1$ in Figs. 6 and 7. We can see that they are not symmetrical, i.e. the increase of n at the local path minimums is slightly larger than its decrease at the local path maximums (this applies for all analyzed cases). Also, the shorter period of case I-2 induces larger overall variations of the n values then in case I-1. Since larger load factors correspond to larger lift forces and consequently larger drag, and vice versa, the applied kind of speed variation generates the average drag increase through the asymmetrical load factor variations. Beside that, if the overall load factor variations are larger due to shorter periods, the average drag increase should also be higher, and thus case I-2 gives 22.2 m larger landing distance reduction than case I-1, although their speed amplitudes are the same.

A general conclusion might be that *higher speed amplitudes* (i.e. departing from the best glide ratio speed towards those that correspond to smaller L/D ratios) *and shorter periods of speed variation are actually the two influence parameters that both contribute to the landing distance reduction*. In here presented final approaches they inherently go together, and they must be combined carefully. Too large speed amplitudes with too short periods can be very unpleasant for the pilot, locally overstress some parts of the sailplane structure and may generally be very dangerous in the vicinity of the ground. Such combinations should be based either on large amplitudes and long periods, small

amplitudes and short periods or moderate amplitudes and moderate periods.

Let us now consider some other important practical aspects of here presented approach profiles. Cases II-1 and II-2, based on initial speed decrease, enable avoiding the 15 m obstacles at practically the same X distances of about 1200 m from the starting point, as in the default case. This is their advantage when obstacles are close to the beginning of the landing ground, since for all cases based on the initial speed increase (I-1, I-2 and I-3) this distance is some 100 to 200 m smaller. On the other hand, the distance reduction obtained by case II-1 of only 26.4 m might be categorized as "too much trouble about nothing" (quite long period and very small departing from $(L/D)_{\max}$), so this case is of rather small practical significance. Quite opposite to that, the case II-2 with almost the same period, gives the second best landing distance reduction of 96 m, owing to the substantial drop of L/D at 60 km/h. It should be noticed that this speed is only some 4 km/h higher than the sailplane's stalling speed, and flying this approach would require caution.

Paths of the cases I-1 and I-2 give moderate ΔX values of 56.7 and 78.9 m, with respect to the maximum achieved $\Delta X = 101.8\,\mathrm{m}$ in case I-3. Although the ground roll phase is not explicitly analyzed in this paper, it should be mentioned that these two profiles have an advantage over the other path profiles considering this aspect. Namely, in case of the high emergency landings on short fields, one of the usual procedures is to try to force the sailplane to the ground at higher speed than nominal (72 km/h in our case) and then start using wheel brake, as a very efficient energy dissipating device. For the Vuk-T sailplane it has been estimated that the speed of 90 km/h could be acceptable top speed limit for such a procedure to be successfully performed. Due to their profiles, cases I-1 and I-2 could enable such forced landings at 90 km/h some 200 m earlier the other presented cases, supposing that the 15 m obstacles are not further than approximately one kilometer from the starting point of the final approach.

The largest distance reduction of 101.8 m has been achieved in case I-3, which looks in a way like a simplified version of the minimized flight path from [1], shown in Fig. 1. It combines a curved path generated by cosine speed variation with large speed amplitude and long period, and a straight path similar to the default case. It is clear that this is just one of many possible combinations, where in this paper the constant speed of 80 km/h for the second portion of the approach has been used intentionally to present the pure contribution of a single path oscillation with such speed amplitude on quite noticeable approach distance reduction. It natural that some other profile choices for the first and second part of the path could give even larger ΔX values.

The distance reductions of the order of 70 to 100 m, compared with the here considered total X distances of about 1.8 km, may not seem very spectacular at the first glance. On the other hand, it must be remembered that sailplane pilots sometimes have no other option but to land on a narrow and quite short countryside field surrounded by trees, power lines, telephone poles, houses, ditches, rivers, etc., and loosing the chance to extend spoilers in such situations makes the last minutes of the flight very critical. In such cases, using some of the relatively simple and quite safe procedures, such as examples given in this paper, to shorten the final approach for a distance which is close to or equal to a football field length, can make a substantial difference between the successful outcome and a disaster. Also, a pilot must not forget to extend the landing gear - not only because it is normal to land a sailplane with the gear down (except on very rough terrains), but also because the extended gear on modern sailplanes causes a drag increase which is far from negligible. If a sailplane pilot can not use spoilers when the approach distance shortening is an imperative, any source of additional drag is extremely valuable.

4 CONCLUSIONS

Two categories of simple cosine speed variations in final approach have been analyzed, as possible ways to reduce the approach distance in cases when spoilers become inoperable. The first category implies that the speed initially increases, and the second that it initially decreases from the reference staring value of 80 km/h at the height of 50 m. For actual calculations the Vuk-T sailplane has been selected. The input values for periods and speed variations have been chosen as rounded and easy-to-remember numbers for practical use, and applied in different ranges

within the two assigned cosine laws. Results were compared with the landing distance of the steady reference path flown at the same speed as at the initial state. Presented examples have been carefully selected to show the influence of those input parameters on possible landing distance reductions, ranging from very small, of the order of 20 m, over moderate 50 to 70 m reductions, to more than 100 m. For all presented cases the initial and the terminal energy states were the same. The oscillating path profiles, simply because they are curved, do not contribute remarkably to the landing distance reduction in any of the treated cases. The analyses have shown that the larger achieved landing distance reductions were actually proportional to the larger speed amplitudes and shorter periods of oscillations, both contributing to the increased energy dissipation. These factors must be combined carefully for operational conditions. Cases involving large speed amplitudes and short periods could be very unpleasant for the pilot and may cause local structural overloading, so this particular combination was not considered.

The so called distance-minimizing techniques, known in literature, are based on very complex oscillating paths in final approach, which would require exceptional piloting skills. On the other hand, the goal of this paper was not to minimize the approach distance for any given sailplane, but to define general influential factors which could be combined within much simpler flying procedures, that can easily and quite safely be performed by pilots of average experience. Although the approach distance reductions obtained by here presented methods are smaller than obtained by distance-minimized approach for the Vuk-T sailplane, under operational conditions they can certainly make the difference between a successful landing and an undesired outcome. Presented principles can readily be applied to any other sailplane for which the required technical data are available.

5 REFERENCES

[1] Stefanović, Z, Cvetković, D. (1996). Minimum landing-approach distance for a Vuk-T sailplane. *20th International Council of Aeronautical Sciences (ICAS) Congress Proceedings*, p. 1061-1064, Sorrento.

[2] Metzger, D.E., Hedrik, J.K. (1975). Optimal flight paths for soaring flight. *Journal of Aircraft*, vol. 12, no. 11, p. 867-871.

[3] Pierson, B.L. (1977). Maximum altitude sailplane winch-launch trajectories. *Aeronautical Quarterly*, vol. 28, p. 75-84.

[4] Ladson, L.S., Waren, A.D., Rice, R.K. (1967). An interior penalty method for inequality constrained optimal control problems. *IEEE Transactions on Automatic Control*, vol.12, IV, p. 388-395.

[5] Pierson, B.L. (1975). Panel flutter optimization by gradient projection. *International Journal for Numerical Methods in Engineering*, vol. 9, p. 271-296.

[6] Roskam, J., Chuen-Tau, E.L. (1997). *Airplane aerodynamics and performance*. DARcorporation, Kansas.

[7] Stefanović, Z, Kostić, I. (2007). Influence of simple harmonic speed variations on the Vuk-T sailplane approach paths and distances. *FME Transactions*, vol. 35, no. 2, p. 15-21.